

Modulation of Amphotericin B Membrane Interaction by Cholesterol and Ergosterol—A Molecular Dynamics Study

Jacek Czub and Maciej Baginski*

Department of Pharmaceutical Technology and Biochemistry, Faculty of Chemistry, Gdansk University of Technology, Narutowicza St 11/12, 80-952 Gdansk, Poland

Received: March 28, 2006; In Final Form: June 16, 2006

Amphotericin B (AmB) is a well-known polyene macrolide antibiotic used to treat systemic fungal infections. According to a well-documented hypothesis, molecules of AmB form ionic membrane channels that are responsible for chemotherapeutic action. These channels disturb the barrier function of the cell membrane which, in consequence, leads to cell death. The presence of sterols in the cell membrane is necessary for full manifestation of the antibiotic's ionophoric activity, at least *in vivo*. Ergosterol-containing fungal membranes are targeted more efficiently by AmB than mammalian membranes containing cholesterol. However, a similar level of disturbance of fungal and mammalian membranes is responsible for serious toxicity of the antibiotic. Due to the importance of AmB and lack of better antifungal alternatives, the search for new less toxic derivatives of this antibiotic still continues. Therefore, studies of the AmB–membrane interaction are very important. The present work constitutes a continuation of a broad program of study on AmB mode of action in our group. In particular, molecular dynamics simulations of AmB monomers inside the bilayers of three different compositions (pure dimiristoylphosphatidylcholine (DMPC) and DMPC bilayer containing ~25 mol % of cholesterol or ergosterol) were carried out. In general, analysis of generated trajectories resulted in identifying many significant differences in the behavior of AmB monomers depending on the membrane environment. In particular, it was established that the antibiotic increases the internal order of DMPC bilayer containing 25 mol % of cholesterol, while it has no effect on the order of the bilayer with the same amount of ergosterol. Performed calculations also revealed that relatively rigid and elongated AmB molecules exhibit higher affinity toward the sterol-containing *lo* phases and, therefore, may be cumulated in ordered membrane domains (e.g., lipid rafts). Since the partition coefficient between the *ld* and *lo* phase appears to be greater in the case of the ergosterol- compared to cholesterol-containing membrane, this effect can be also discussed as the possible origin of AmB-selective toxicity and indirect sterol involvement in expression of AmB activity.

Introduction

Amphotericin B (AmB) is a well-known polyene macrolide antibiotic that has been successfully used, as a life saving drug, to treat systemic fungal infections for over 45 years.^{1,2} The chemical structure of AmB (Figure 1) is rather complex, and it consists of (i) a planar elongated macrolide ring containing a rigid heptaene fragment in one part and a polyol chain in another one and (ii) the so-called polar head containing a carboxyl group and a mycosamine moiety.

Despite a long history of medicinal application, the mechanism of AmB's action has not been yet determined. However, it is commonly accepted that antibiotic molecules form ion channels in the cell membrane, leading to disturbances in physiological ion and small solute transmembrane flows. As a consequence, this transportation impairment can cause cell death. Furthermore, numerous experimental studies on different cell and model lipid membrane systems (including very simple bilayers containing only one type of glycerophospholipid) revealed that AmB's ionophoric action is to a large extent sterol-dependent. This means that AmB needs the presence of sterols in the membrane for full manifestation of its channel activity.^{3,4} According to these studies chemotherapeutic application of the antibiotic is possible due to the higher ability of AmB to impair

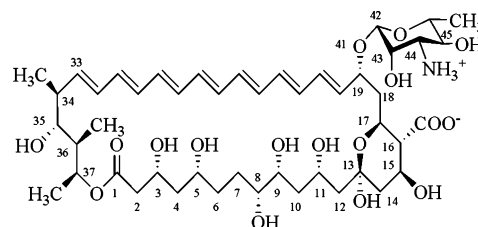


Figure 1. Chemical structure of amphotericin B (AmB).

the function of membranes containing ergosterol (Erg), principal fungal sterol, compared to membranes with cholesterol (Chol), to be found in mammalian cells.^{5–7} Unfortunately, as a result of only quantitative differences of the activity in both types of membranes, AmB is highly toxic, particularly nephrotoxic.^{8,9} On the other hand, lack of better antifungal alternatives as well as a variety of favorable chemotherapeutic properties (e.g., very wide antifungal spectrum and lack of induction of secondary resistance) make AmB a very promising lead compound for rational design of novel, more selective antifungals.^{10,11} However, a still insufficient understanding of the molecular origin of the antibiotic's selective toxicity constitutes the main obstacle in developing new less toxic derivatives of AmB.

There are two hypotheses to explain the quantitative selective toxicity of AmB against cells containing Erg in their membranes. First, the more classical hypothesis, it is assumed that the polyene molecules interact *directly* with sterol molecules present

* To whom correspondence should be addressed. Phone: +48-58-3471596. Fax: +48-58-3471144. E-mail: maciekb@hypnos.chem.pg.gda.pl.

in the membrane and form so-called 'primary complexes'. Subsequently, such complexes associate in the so-called 'barrel-stave channel'. In this model AmB selectivity arises from its higher affinity toward Erg than Chol.^{3,12} The second hypothesis presumes that only *indirect* action of sterol molecules is responsible for differentiation of AmB's ability to form stable channels in the Erg- or Chol-containing membranes. In this case, selectivity of AmB is an effect of different modulation of the lipid bilayer properties by both types of sterols. Diverse properties of the lipid bilayer may cause, for instance, differences in the capability of AmB to enter the membrane or differentiate behavior of the antibiotic molecules inside the membrane.^{13–15}

The aim of our work was to probe mainly the second above-mentioned hypothesis. To this end, *in silico* models of the lipid membrane, previously elaborated and tested,¹⁶ were applied to study interaction of AmB molecules with lipid bilayers. In the present study we analyze various properties and interactions of AmB monomers embedded in a pure phospholipid bilayer and in Chol- and Erg-containing bilayers. Several experimental reports demonstrated that AmB can exist in the monomeric state inside the membrane.^{17,18} In the simplest model of channel activity, these monomers (or possibly preformed AmB:sterol primary complexes) subsequently associate in the barrel-stave structure.^{17,19–21} However, it is still not known at which stage of this mechanism the selectivity appears.

To study the molecular aspects of AmB's mechanism of biological action we applied the molecular dynamics (MD) technique. Our work, to the best of our knowledge, is the first MD simulation of AmB molecules within their molecular target, namely, the lipid membrane. Thus, our approach should help to clarify how the composition of the lipid bilayer influences the behavior of AmB monomers. Specifically, the analysis of simulation data was expected to show some molecular explanation for (i) the observed dependence of AmB's *activity* on the presence of sterols and (ii) the *selectivity* exhibited by antibiotic in both sterol-containing membranes.

As far as application of MD in our project is concerned, it is worth mentioning that during the past decade classical molecular dynamics (MD) simulations have proved to be a valuable approach in studying lipid bilayers and their interactions with small solutes and biopolymers.^{22,23} In particular, simulations were carried out to investigate the influence of certain drugs (especially anesthetics) on the properties of phospholipid bilayers^{24,25} as well as examine different structural and dynamic properties of antimicrobial peptides embedded within a lipid membrane.^{26,27} This technique was also used in our previous projects concerning lipid membranes and AmB membrane channels.^{20,21,28}

In the present study MD simulations of AmB monomers inside the bilayers of three different compositions (pure dimyristoylphosphatidylcholine (DMPC) and DMPC bilayer containing ~25 mol % of Chol or Erg) were carried out. In general, analysis of generated trajectories resulted in identifying many significant differences in the behavior of AmB monomers depending on the membrane environment.

It is also worth mentioning that our study for the first time reveals at the molecular level the effect of sterol composition on differentiation of various properties of membrane-embedded ligand. Thus, this work might be of general importance for understanding molecular aspects of chemotherapy targeted at the cell membrane. It is also an example showing that application of molecular dynamics to study lipid membranes shifts to a new era beyond just a simple reproduction of experimental

results. In our case, the simulations provide new knowledge, which can help to understand and explain the mechanism of action of a membrane-active ligand/drug.

Methods

1. Simulated System. Three comparative molecular dynamics (MD) simulations were performed with respect to the systems containing AmB monomers embedded in the pure DMPC bilayer and in the DMPC bilayer containing ~25 mol % of Chol or Erg (referred as DMPC/AmB, DMPC/Chol/AmB, and DMPC/Erg/AmB systems, respectively). The initial structures of the simulated systems were prepared using final configurations obtained in the previously reported¹⁶ MD simulations of the membranes composed of 128 DMPC molecules and, in the case of mixed bilayers, 42 Chol or Erg molecules. All these three bilayers were equilibrated and fully hydrated with 5278 water molecules. To achieve better statistics, 12 and 8 monomers of AmB were introduced into the pure and sterol-containing bilayers, respectively. The number of AmB molecules in the DMPC/AmB system was higher to facilitate analysis of the influence of monomeric AmB on the properties of pure phospholipid bilayers. Antibiotic molecules were placed inside the membranes in a sequential way. At each step of the placing procedure, first, the cavity of roughly cylindrical shape was formed at a randomly chosen location of the selected leaflet. This was done by performing a relatively short (0.5–1 ns) MD simulation in the NPT ensemble with external harmonic forces directed along the normal to the surface of the defined cylinder and acting on all the atoms that are located inside this cylinder. The radius of the cylinder was systematically changed from 0 to 0.4 nm. A similar method was previously used for membrane proteins and peptides.²⁹ The AmB molecule was then put into the cavity in a manner corresponding to its ionophoric mechanism of action, that is with the polar head positioned at the water/bilayer interface and the large lactone ring buried within the membrane hydrocarbon core. The initial, low-energy geometry of the AmB monomer was taken from the formerly reported conformational analysis.³⁰ After molecule insertion the energy minimization procedure was carried out to remove possible bad van der Waals contacts (positions of AmB atoms were kept fixed during this stage). The same number of antibiotic molecules was introduced in the way described above into each leaflet of the individual systems.

2. Simulation Details. All energy minimizations and MD simulations were carried out using the GROMACS package.³¹ The topology and force field parameters for DMPC molecules were based on the commonly used united-atom parameter set for dipalmitoylphosphatidylcholine (DPPC).³² The parametrization of Chol and Erg molecules was the same as that employed in previous works.^{16,33} It should be mentioned here that these simulation studies, also using Berger et al. parameters for phospholipids,³² were successful for reproducing numerous measurable parameters of binary membrane systems. Force field parameters (except partial charges) and topology for the AmB molecule were generated using the PRODGR server (<http://davapc1.bioch.dundee.ac.uk/programs/prodgr/>).³⁴ The same set of atomic charges for AmB were used as in our previous works.^{21,28,35} These charges were obtained by fitting to the electrostatic potential generated by the molecule.³⁶ Similarly to DMPC and sterol molecules, the united atom approach was applied for all nonpolar CH_n groups of AmB. As a result, only polar hydrogen atoms were kept explicitly in the antibiotic molecule.

To eliminate edge effects, three-dimensional periodic boundary conditions were applied in all simulations. Electrostatic

interactions were calculated using the smooth particle mesh ewald summation method (SPME)³⁷ with a real space cutoff of 0.9 nm and a fast Fourier transform grid spacing of approximately 0.1 nm in all three dimensions. van der Waals interactions within 0.9 nm were evaluated every MD step, and interactions between 0.9 and 1.2 nm were determined every 10 steps. The pair list for short-range nonbonded interactions was updated every 10 MD steps. To make it possible to use a longer time step all covalent bonds in the system were constrained to their reference values with the LINCS algorithm³⁸ for phospholipid, sterol, and antibiotic molecules and with the SETTLE scheme³⁹ for water.

Equations of motion were integrated using the leap frog Verlet algorithm with an integration step of 2 fs. The temperature and pressure were maintained around 300 K and 1 bar by means of the Berendsen weak coupling method⁴⁰ with time constants of 0.1 and 1.0 ps, respectively. To counteract possible formation of temperature gradients, temperature coupling was applied separately to solvent and lipid molecules. The size of the simulation box was allowed to adjust independently in all three space directions. Since the applied external pressure was isotropic (1 bar in all three directions), the equilibrium state of the membrane should correspond to zero surface tension value (NPT ensemble).

All three systems were simulated for 40 ns; atom coordinates were stored every 2 ps. The last 30 ns of each run was then regarded as a productive simulation and taken to analysis of different system properties. The simulations were performed on four nodes of 1.3 GHz Itanium 2 cluster with a performance of ~36 ps per hour of CPU time.

The total energy, its components, and dimensions of the simulation cell were monitored (data not shown), and the equilibration time employed seemed to be sufficient to obtain reasonable convergence for most of the properties that were of interest during the analysis stage. The final configurations of the simulated systems are shown in Figure 2.

Results and Discussion

Analysis of MD trajectories of the systems containing AmB monomers embedded in the DMPC bilayer (both pure and containing ~25 mol % of Chol or Erg) was focused on the comparison of various structural and dynamic properties of antibiotic molecules as well as their interactions in different membrane environments.

1. AmB Localization and Orientation. To characterize the preferred localization of AmB molecules within the membrane we calculated the electron density profiles (EDP) of selected functional groups across the lipid bilayer (Figure 3). Both pure and sterol-containing initial DMPC membranes, utilized in this study to prepare the systems with AmB, were previously shown to provide EDP in good agreement with the experimental data.¹⁶ If we define the bilayer thickness as the distance between the maxima of electron density of phosphate groups coming from both leaflets (3.63, 4.37, and 4.42 nm in the DMPC/AmB, DMPC/Chol/AmB, and DMPC/Erg/AmB systems, respectively), it can be observed that in the thicker sterol-containing membranes antibiotic molecules reside solely in one membrane layer. This is an expected result since AmB's polar heads seem to be strongly attached to the water/membrane interface (see also the Intermolecular Interactions section) and their molecular length is only about 2.5 nm, which does not allow spanning both leaflets of the membrane. On the other hand, in the considerably thinner pure DMPC membrane AmB molecules penetrate in a significant way the other membrane leaflet. The electron density

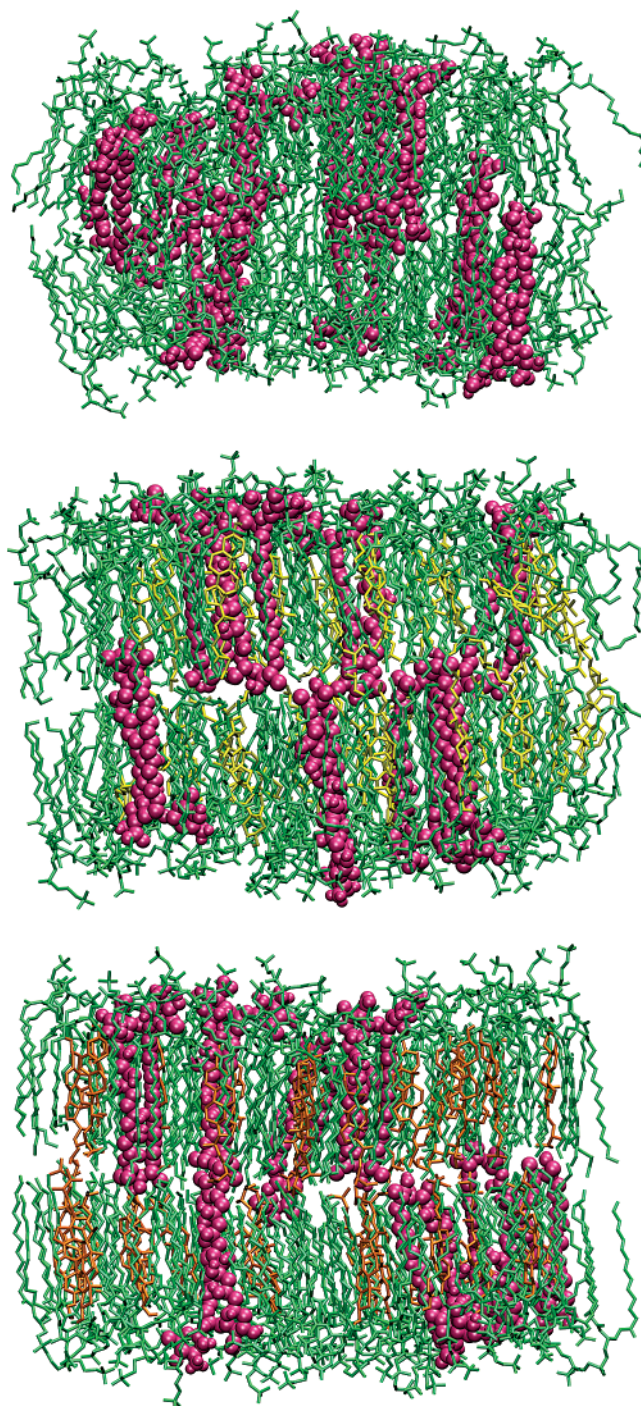


Figure 2. Final MD frames of DMPC/AmB (top), DMPC/Chol/AmB (middle), and DMPC/Erg/AmB (bottom). Phospholipid and sterol molecules are presented as stick models (DMPC, green; Chol, yellow; Erg, orange). AmB is shown as a CPK model. For the purposes of clarity, water molecules were omitted.

distribution of the AmB 35-hydroxyl (35-OH) group in this system partly overlaps with the distributions corresponding to the carbonyl and (even) phosphate (PO_4^-) groups of DMPC. Since the AmB molecules themselves can, to some extent, increase the membrane thickness (see the Influence on Membrane Properties section), it seems that with a lower antibiotic content this overlapping would be even higher. Finding that the AmB molecule is able to span the DMPC membrane is consistent with the results of ^{13}C NMR studies using ^{13}C -labeled antibiotic.⁴¹ This suggests that AmB molecules should presumably be able to form the so-called single length channels in

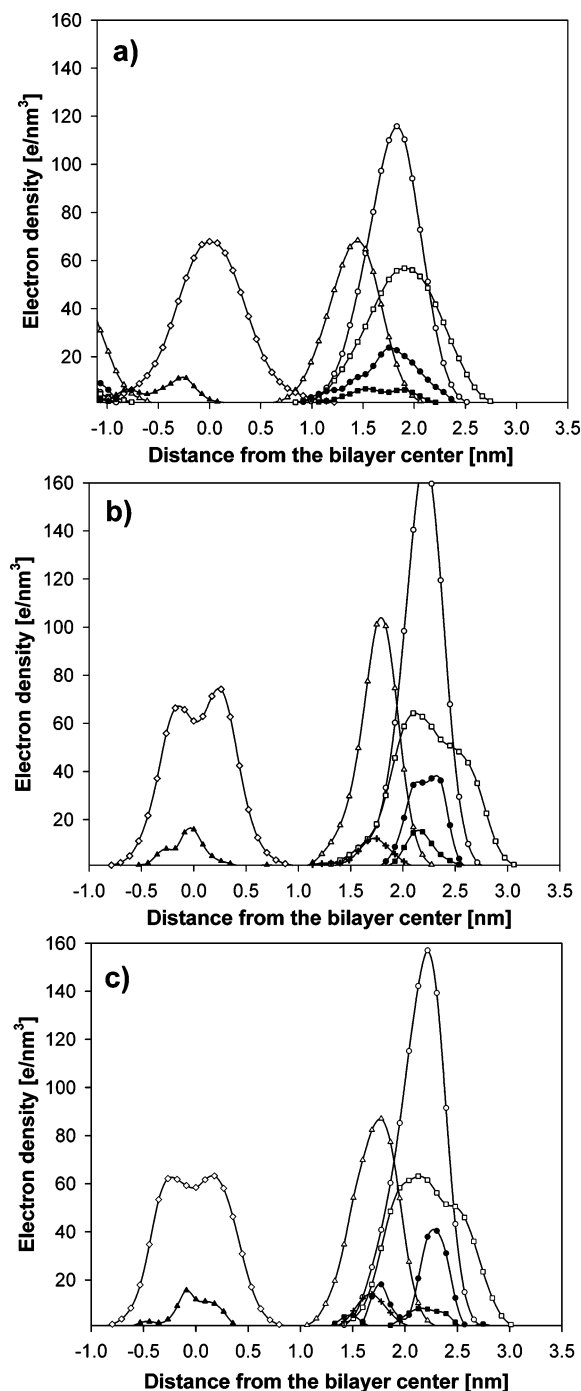


Figure 3. Electron densities of selected groups across the DMPC/AmB (a), DMPC/Chol/AmB (b), and DMPC/Erg/AmB (c) bilayers: trimethylammonium groups (\square), phosphate groups (\circ), carbonyl groups (Δ), DMPC terminal methyl groups (\diamond), sterol hydroxyl groups ($+$), AmB carboxyl group (\bullet), AmB amino group (\blacksquare), and AmB hydroxyl-35 group (\blacktriangle). To facilitate the analysis of presented data, the EDPs for AmB groups were arbitrarily multiplied by a factor of 7.

membranes of thickness comparable to the one observed in the pure DMPC bilayer. However, many other experimental studies have demonstrated that under normal conditions and at low (i.e., therapeutic) concentrations AmB does not permeabilize sterol-free DMPC membranes in their fluid state.^{12,42} Therefore, there must be some other determinants of the AmB's ionophoric activity different than simply the thickness of the lipid bilayer. On the other hand, if one assumes that chemotherapeutically relevant AmB ion channels are formed within the sterol-induced liquid-ordered (*lo*) membrane phases,⁴³ then our results (Figure

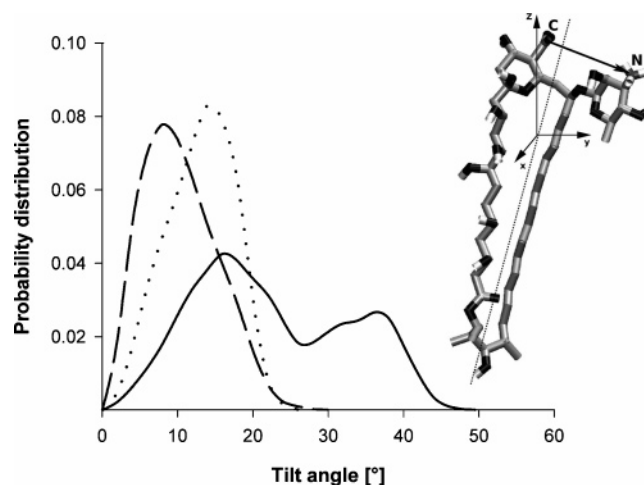


Figure 4. Distributions of the AmB tilt angles (angle between the longest principal axis of AmB and the normal to the bilayer plane) calculated in the DMPC/AmB (solid line), DMPC/Chol/AmB (dashed line), and DMPC/Erg/AmB (dotted line) systems. Additionally, the schematic view of AmB molecule is shown with its principal axis presented as a dashed line and headgroup dipole moment depicted as a vector connecting the negatively charged carboxyl group and positively charged amino group.

3) may indicate that the double length channel is a more probable channel structure.

Concerning the position of the AmB polar head at the membrane interface, it is apparent that in all the cases distribution (Figure 3) corresponding to the negatively charged carboxyl group (COO^-) is shifted a little toward the water phase, compared to the protonated amino group (NH_3^+). This may suggest that the AmB polar head dipole ($\text{COO}^- \rightarrow \text{NH}_3^+$) tends to “match electrostatically” dipole potential coming from phosphatidylcholine headgroup dipoles ($\text{PO}_4^- \rightarrow \text{NMe}_3^+$, where NMe_3^+ denotes the trimethylammonium group). The latter dipoles are, on average, oriented in such a way that they produce an outwardly directed, nonzero component of the dipole moment in the direction perpendicular to the membrane surface.^{16,44} This effect can be also observed in Figure 3, where distributions corresponding to NMe_3^+ groups are located at a distance from the membrane center a bit longer than PO_4^- distributions.

Due to the presence of seven conjugated double bonds in the lactone ring, the AmB molecule constitutes a rather elongated and relatively rigid structure. Hence, it is possible to define a vector specifying the orientation of the whole antibiotic molecule with respect to the bilayer surface. The average tilt of polyene molecules, defined as the angle between the membrane normal (the z axis) and the vector directed along the longest principal axis of AmB (that is, the eigenvector corresponding to the smallest eigenvalue of the inertia tensor calculated with respect to the center of mass of the molecule), was examined in each of the simulated systems (Figure 4). It is evident that addition of a physiological amount of both sterols to the pure DMPC membrane causes a large change in the average orientation of AmB molecules, making it much more perpendicular to the membrane surface. The width of the tilt angle distribution, characterizing the range of the allowed orientations, is also reduced in the sterol-containing membranes. These findings are consistent with the results of a study by Lopes and Castanho¹³ employing UV-vis linear dichroism spectroscopy. They showed in their work similar changes in the average AmB orientation upon addition 33 mol % of Chol to aligned DPPC multilayers.¹³ Since relatively long (tens of nanoseconds) MD simulations of lipid bilayers are known to give a reasonable

sampling of local structural properties, it seems that the bimodal distribution obtained in the DMPC/AmB system may in fact reveal the existence of two different preferred orientations of the polyene molecule in a sterol-free phospholipid bilayer (maxima of probability density at $\sim 18^\circ$ and $\sim 37^\circ$). A significant change in the average alignment of AmB molecules inside the membrane observed under the influence of sterols most likely arises from the ability of these molecules to increase the conformational order of the membrane hydrocarbon region.^{16,45,46} In the highly ordered and packed sterol-containing membranes, where the majority of phospholipid acyl chains are most of the time oriented along the membrane normal, the possibility for antibiotic molecules to deviate from approximately vertical alignment is strongly limited. On the other hand, the general tendency of AmB to diverge from this orientation, visible, e.g., in the DMPC/AmB system, appears to result from the above-mentioned electrostatic matching of the AmB and lipid headgroup dipoles. Since the mutual space arrangement of the mycosamine ring and the aglicon part was previously shown to be fairly stable,^{28,30} this dipole matching is often possible only by deflection of the whole molecule from the orientation perpendicular to the membrane surface (see also schematic drawing in Figure 4).

The differences seen in the average alignment of AmB monomers inside sterol-free and sterol-containing bilayers can be interpreted in light of the classical, channel mechanism of AmB action. It seems that ensuring a stable vertical position inside the membrane as well as reducing fluctuations of mutual orientation of associating polyene molecules should favor the effectiveness of aggregation into the barrel-stave channel. One could furthermore argue that the condensed and relatively rigid sterol-containing lipid bilayers (e.g., the liquid-ordered membrane domains) are the environment appropriate for formation of stable supramolecular structures, such as the AmB channel. Therefore, our results support the conjecture that membrane sterols activate expression of AmB's ionophoric action by their ability to modulate the properties of the bilayer, particularly by a condensing and ordering effect on phospholipid molecules.

2. Influence on Membrane Properties. To determine whether the AmB molecules have an effect on the structure of a one-component phospholipid bilayer, we calculated a few commonly analyzed parameters for the DMPC/AmB system. Figure 5a displays the order parameter profiles of the *sn*1 and *sn*2 DMPC acyl chains in the DMPC/AmB system and in the pure DMPC bilayer. The latter profiles were taken from our previous work, where they were shown to be in quantitative agreement with experimental data.¹⁶ The deuterium order parameter, S_{CD} , often used as a measure of orientational order of lipid acyl chains, is readily obtained in H^2 NMR experiments as well as from MD simulations. For a given methylene group it may be defined as

$$S_{CD} = \left\langle \frac{3}{2} \cos^2 \beta - \frac{1}{2} \right\rangle \quad (1)$$

where β is the angle between the C–D (or C–H) bond vector and the bilayer normal. Since we employed the united atom model to calculate the order parameter in a direct way we had to assume a tetrahedral geometry of all methylene groups. For every methylene group averaging was done over both C–H bonds, all the lipid molecules, and the simulation time. The calculated S_{CD} values, presented in Figure 5a as a function of carbon atom number, clearly indicate that addition of ~ 8.6 mol % of AmB to DMPC bilayer significantly increases the conformational order of the phospholipid acyl chains. The effect

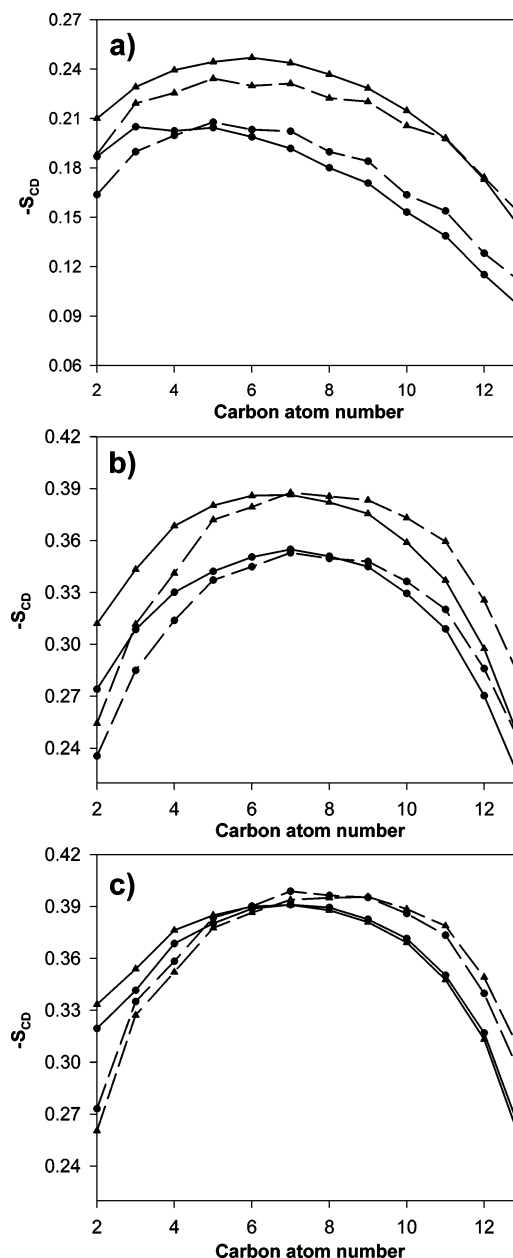


Figure 5. Profiles of the deuterium order parameter calculated for the DMPC *sn*-1 (solid line) and *sn*-2 (dashed line) acyl chain in the DMPC/AmB (a), DMPC/Chol/AmB (b), and DMPC/Erg/AmB (c) systems. In addition to order parameter values calculated for AmB-containing systems (\blacktriangle) we present profiles obtained in similar systems without antibiotic molecules (\bullet).¹⁶

of the improved packing upon insertion of AmB is also confirmed by calculation of other parameters, correlated to some extent with the S_{CD} , such as the bilayer thickness and the area per one phospholipid molecule. Straightening of acyl chains is usually accompanied by the increase of the membrane thickness. Indeed, the distance between the maxima in the overall EDP plot, D_{HH} , which is often used as the definition of the bilayer thickness, is significantly larger in the DMPC/AmB system (3.41 nm) than in the pure DMPC system simulated by us in the previous study (3.30 nm).¹⁶ If we assume that the membrane area per (relatively rigid) AmB molecule is equal to the molecular area estimated in the antibiotic monolayer in which molecules were oriented perpendicularly to the air/water interface (0.55 nm^2),⁴⁷ it is possible to divide the total membrane area in the DMPC/AmB system between phospholipid and antibiotic molecules in the same manner as it was previously

done for sterol-containing bilayers.^{48,49} Subtracting from the total area of the bilayer ($2 \times 41.28 \pm 0.652 \text{ nm}^2$) the area occupied by AmB molecules ($12 \times 0.55 \text{ nm}^2$) and dividing the obtained difference by the number of DMPC molecules, we finally get $0.593 \pm 0.010 \text{ nm}^2$ as the area per DMPC molecule in the mixed system. This value, smaller than in pure DMPC system ($0.618 \pm 0.0083 \text{ nm}^2$), confirms the condensing effect of polyene molecules on a phospholipid bilayer. Ordering and condensing action of AmB on lipid membranes can be explained by the fact that the polyene molecule and especially its macrolide part is, similarly to sterols, characterized by a rather rigid structure and a relatively smooth molecular surface. Maximization of van der Waals interactions between such molecules and membrane lipids leads to ordering (straightening) of the lipid acyl chains and, as a result, condensation and rigidification of the bilayer. The strong ordering effect of AmB on phospholipids (even greater than the one made by similar concentration of Chol³³) may suggest that formation of membrane domains/clusters enriched with AmB, which was observed experimentally,⁵⁰ can proceed in a way similar to the sterol-induced separation of the *lo* phases.⁵¹

Interesting conclusions can also be drawn by comparing the S_{CD} profiles calculated for the DMPC/Chol/AmB and DMPC/Erg/AmB systems (Figure 5b and c). Particularly, it can be noticed that while AmB present in the Chol-containing membrane causes an additional increase of the internal membrane order, no such effect is observed in the Erg-containing system. In fact, the S_{CD} values in this bilayer are almost the same independent of the antibiotic's presence. Such a result is most likely due to a high degree of ordering already introduced by 25 mol % of Erg.¹⁶ Nearly complete stretching of DMPC hydrocarbon chains along the bilayer normal in the DMPC/Erg system precludes an additional condensation under the influence of other "order-inducing" molecules such as AmB.

If one assumes that full expression of the channel-forming activity of AmB requires a sufficient degree of membrane conformational order, then the differences observed in the S_{CD} profiles of both sterol-containing bilayers could be interpreted in terms of antibiotic selectivity. It is known that AmB's selectivity of action, that is, stronger permeabilization of Erg-containing membranes than Chol-containing ones, is manifested only at low antibiotic concentrations (much lower than the concentration applied in our work (1:16 AmB:DMPC)). This means that higher concentrations of AmB are necessary to obtain the same activity in membranes with Chol than with Erg.^{42,52} Therefore, it may be proposed that the level of a bilayer order necessary for stable channel formation should be achieved easier in more condensed Erg-containing membranes. On the contrary, obtaining this level in Chol-containing bilayers may require higher AmB concentration.

3. Dynamic Properties of AmB. Variations in the dynamic behavior of AmB monomers inside the membrane, depending on the presence and/or type of sterol, may also be significant for antibiotic activity and selectivity. To characterize these differences, we first examined the overall rotational motion of AmB molecules inside each of the studied bilayers. To this end, reorientational autocorrelation functions of certain vectors were calculated

$$C(t) = \langle P_2[\mathbf{r}(t_0 + t)\mathbf{r}(t_0)] \rangle = \frac{3}{2} \langle [\mathbf{r}(t_0 + t)(t_0)]^2 \rangle - \frac{1}{2} \quad (2)$$

where $\mathbf{r}(t_0)$ and $\mathbf{r}(t_0 + t)$ is a unit vector defining given rotational motion in the initial time, t_0 , and after the time t , respectively. Averaging was done over all antibiotic molecules and all

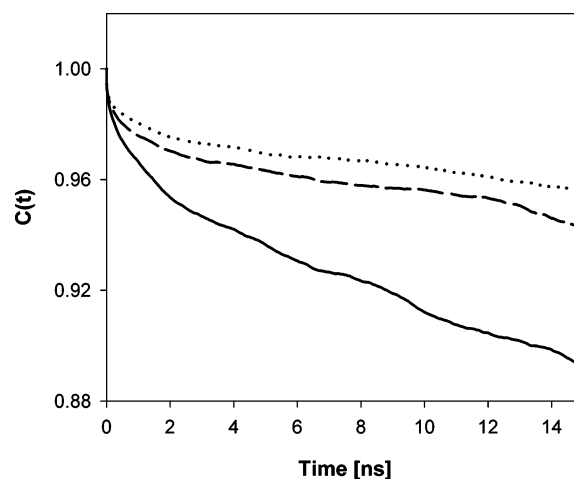


Figure 6. Time autocorrelation functions of the vectors directed along the longest principal axis of the AmB molecule obtained from simulation of the DMPC/AmB (solid line), DMPC/Chol/AmB (dashed line), and DMPC/Erg/AmB (dotted line) systems.

possible initial times, t_0 . To obtain the time evolution of unit vectors describing different rotational modes of AmB, the moment of inertia tensor of AmB with respect to the molecule center of mass was calculated for every MD frame. The eigenvector corresponding to the smallest eigenvalue was then taken to define the so-called wobbling motion of the antibiotic molecules, that is, the motion corresponding to changes of the angle between the AmB longest principal axis and the bilayer normal. The time autocorrelation functions of this vector, calculated in the three simulated systems, are presented in Figure 6. The relatively slow decay of these curves visible for all the systems indicates the occurrence of a strong restriction imposed on the reorientational motion of the AmB's longest axis inside the phospholipid membrane. Despite the fact that none of the curves reaches its plateau value, which is related to the generalized order parameter,⁵³ it is obvious that in more densely packed sterol-containing membranes the AmB wobbling motion is restricted more strongly. This restriction is slightly more pronounced in the bilayer containing Erg molecules, which are known to produce a more compact membrane environment than Chol molecules do. To quantitatively compare the ability of the three studied membrane systems to align polyene molecules along the bilayer normal (a factor that is postulated to play an important role in the AmB channel formation process and/or in stabilization of the channel already formed), we can assume that the values of $C(t)$ functions at 15 ns are equal to the square of the generalized order parameter, S^2 .⁵³ We can now consider a simple model of AmB dynamics, namely, the model of a rigid rod fastened at one end (the membrane interface) and diffusing (changing the tilt angle with respect to the bilayer normal) according to the following potential

$$U(\theta) = -fP_2(\cos \theta) = -f\left(\frac{3}{2} \cos^2 \theta - \frac{1}{2}\right) \quad (3)$$

where θ is the angle between the rod axis and the bilayer normal and f is a constant determining the strength of the field. In this case, the order parameter, S , can be obtained by averaging the $P_2(\cos \theta)$ over the potential

$$S = \langle P_2(\cos \theta) \rangle = \frac{\int_0^{\pi/2} P_2(\cos \theta) \exp(-U(\theta)/kT) \sin \theta d\theta}{\int_0^{\pi/2} \exp(-U(\theta)/kT) \sin \theta d\theta} \quad (4)$$

where k and T are the Boltzmann constant and absolute temperature, respectively. Calculating the integrals on the right-hand side of eq 4 at a temperature of 300 K, we obtain a relation between the constant f and the order parameter. Numerical solution of this equation with respect to f for the three different S values coming from our simulations (calculated as the square root of the wobbling correlation functions at $t = 15$ ns) gives a field strength of 18.2, 34.9, and 45.7 kT in DMPC/AmB, DMPC/Chol/AmB, and DMPC/Erg/AmB, respectively. Thus, these values confirm our previous finding that both sterol-doped membranes are able to stabilize the vertical arrangement of antibiotic molecules in a more effective manner. Moreover, the fungal sterol seems to influence the antibiotic orientation to an extent higher than the human equivalent. It is also worth noticing that this difference could be even more pronounced if we simulated the single AmB monomer. In this case, we would avoid the influence of the rest of antibiotic molecules on the ordering of lipid acyl chains in the Chol-containing system and, consequently, on membrane ability to orient AmB molecules (see Figure 5). The autocorrelation functions shown in Figure 6 can also be used to estimate differences in the rate of AmB wobbling motion in the three studied lipid environments. To describe the kinetics of the $C(t)$ decays, we fitted the individual curves to a sum of exponentials of the following form

$$C(t) = a_0 + \sum_{i=1}^n a_i \exp(-t/\tau_i) \quad (5)$$

where fitting parameters τ_i and a_i are correlation times corresponding to different time-scale components of the rotational motion and their amplitudes, respectively. It was proposed that the considered reorientational motion is better characterized by the average relaxation time⁵⁴

$$\tau_m = \left(\sum_{i=1}^n a_i \right)^{-1} \sum_{i=1}^n \tau_i a_i \quad (6)$$

than the individual correlation times, τ_i . Taking $n = 3$ (similarly as in the analytical approximation of $C(t)$ for the wobbling motion of a rigid rod⁵⁵) we obtained the following values for τ_m : 24.0 ± 0.5 , 28.1 ± 2.1 , and 29.5 ± 1.8 ns in the DMPC/AmB, DMPC/Chol/AmB, and DMPC/Erg/Am systems, respectively. Since all these relaxation times are longer than the time for which the $C(t)$ function was calculated, their values are rather rough estimations and any comparison between them should be made with caution. Nevertheless, a comparison of the estimated relaxation times with the values obtained in the same way for DMPC molecules (4.32 ± 0.02 , 4.83 ± 0.01 , and 3.86 ± 0.01 ns in DMPC/AmB, DMPC/CHOL/AmB, and DMPC/ERG/AmB, respectively) shows that AmB molecules, irrespective of the membrane composition, wobble with a rate 1 order of magnitude lower than the more flexible phospholipid molecules.

Subsequently, we analyzed the translational diffusion of AmB molecules embedded in three different membrane environments. To quantitatively describe the lateral (in plane of the membrane) diffusion of the antibiotic molecules, we calculated the corresponding mean square displacements (MSD) as a function of time

$$\text{MSD}(t) = \langle [x(t_0 + t) - x(t_0)]^2 + [y(t_0 + t) - y(t_0)]^2 \rangle \quad (7)$$

where $x(t)$ and $y(t)$ are the coordinates of the AmB center of mass (COM) at time t and averaging is done over all antibiotic

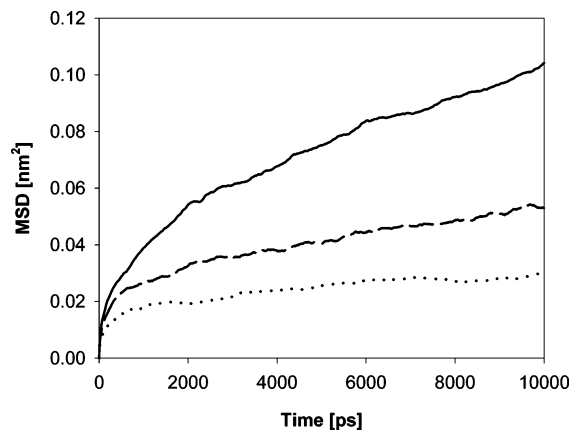


Figure 7. Lateral mean square displacements of the center of mass of AmB monomers in the DMPC/AmB (solid line), DMPC/Chol/AmB (dashed line), and DMPC/Erg/AmB (dotted line) systems.

molecules and all possible initial times, t_0 . To prevent overestimation of the MSDs, the displacements in each membrane leaflet were calculated after removing the COM motion of this layer. The resulting MSD functions are presented in Figure 7. It can be seen that, on the simulated time scale, AmB molecules did not diffuse very far from their initial positions. It is also evident that the displacement was larger in the case of the liquid-disordered (*ld*) phase in the DMPC/AmB system (the root-mean-square displacement in this system was 0.32 nm vs values of 0.23 and 0.17 nm in the case of the DMPC/Chol/AmB and DMPC/Erg/AmB systems, respectively). Assuming a diffusive model for the lateral motion, we could further utilize the calculated MSD functions to estimate the lateral diffusion constants, D , of AmB molecules inside the simulated bilayer systems according to Einstein's equation

$$D = \lim_{t \rightarrow \infty} \frac{1}{4} \frac{d}{dt} (\text{MSD}(t)) \quad (8)$$

where long-time slope was estimated by fitting a straight line to the last 5 ns of each curve. Values of $(1.85 \pm 0.064) \times 10^{-8}$, $(7.94 \pm 0.031) \times 10^{-9}$, and $(3.65 \pm 0.023) \times 10^{-9}$ cm²/s for D were obtained in the DMPC/AmB, DMPC/Chol/AmB, and DMPC/Erg/AmB systems, respectively. To the best of our knowledge, there are no experimental data on the lateral diffusion of polyene antibiotics. However, our results indicate that the diffusion constants of AmB for all three studied systems are about 1 order of magnitude smaller than the values measured and calculated for phospholipid and sterol molecules.^{16,56,57} Since the dimensions of AmB and phospholipid molecules are quite similar and, in addition, a more rigid structure of AmB should rather promote the lateral mobility (compared to the flexible phospholipid structure with tendencies to entanglement), the differences detected between the diffusion constants most probably arise from stronger interactions of the antibiotic with adjacent molecules in the interfacial region of the membrane. Due to the presence of polar hydrogen atoms in its headgroup, AmB, as distinguished from phosphatidylcholines, is able to participate as a donor in formation of intermolecular hydrogen bonds with polar functional groups of other molecules. It is also possible to see that the value of the AmB diffusion constant depends on the membrane composition. Namely, this constant decreases with an increase of membrane rigidity. This is certainly an expected tendency since bilayer condensation results in both a reduction of amplitudes of "rattling motion" in the cage of neighboring molecules and increasing of the "cage-to-cage jump" activation barrier.⁵⁷

TABLE 1: Average Number of Hydrogen Bonds (per one AmB molecule) Formed between the Antibiotic Polar Functional Groups and Different Acceptors of DMPC Molecules

AmB group	DMPC group		
	PO ₄ ⁻	<i>sn</i> -1 C=O	<i>sn</i> -2 C=O
DMPC/AmB system			
NH ₃ ⁺	0.99	0.07	0.24
OH-45	0.11	0.04	0.11
OH-43	0.10	0.04	0.03
OH-15	0.07	0.04	0.04
OH-13	0.03	0.02	0.03
DMPC/Chol/AmB system			
NH ₃ ⁺	0.96	0.04	0.16
OH-45	0.14	0.02	0.06
OH-43	0.10	0.04	0.03
OH-15	0.07	0.04	0.04
OH-13	0.03	0.02	0.03
DMPC/Erg/AmB system			
NH ₃ ⁺	0.98	0.19	0.27
OH-45	0.11	0.03	0.06
OH-43	0.07	0.09	0.06
OH-15	0.05	0.03	0.02
OH-13	0.01	0.04	0.01

4. Intermolecular Interactions. Intermolecular noncovalent interactions are presumed to be a very important factor in the AmB-induced permeabilization of the cell membrane. The significance of these interactions results from the fact that they govern the geometry and energetics of different supramolecular complexes of antibiotic molecules inside the lipid membrane (including ion channel structures).^{19–21}

As a molecule containing many polar functional groups, AmB is able to form intermolecular hydrogen bonds acting as either a donor or an acceptor. Using a simple geometric criterion for the presence of a hydrogen bond (namely, the distance between donor, D, and acceptor, A, should be shorter than 0.35 nm and the angle between the vector connecting D with A and the bond D–H should be smaller than 60°) we monitored the formation of hydrogen bonds between AmB polar groups and different accepting sites of DMPC molecules (DMPC essentially cannot participate in hydrogen-bond formation as a donor). Table 1 contains the number of bonds between polar groups of antibiotic and DMPC molecules averaged over the generated ensemble of configurations. The most striking aspect of these results is that, irrespective of the system, the AmB NH₃⁺ group is involved in the specific interaction with the PO₄⁻ group of DMPC molecules. The stability of this, often bifurcated, hydrogen bond is additionally increased by the favorable electrostatic interactions between the PO₄⁻ and NH₃⁺ groups bearing opposite charge. Further inspection of the trajectories reveals that nearly all antibiotic molecules were connected with only one DMPC molecule throughout the entire simulated period (i.e., the lifetime of the observed interactions was relatively long). The existence of rather stable complexes of AmB and saturated phospholipid (DMPC and DPPC) molecules was previously postulated on the basis of ¹³C–³¹P intermolecular dipolar coupling measurements⁴¹ and monolayer studies.⁵⁸ The results of our simulations indicate that the specific NH₃⁺–PO₄⁻ interaction may be the main factor contributing to stabilization of these complexes. Moreover, it seems that the most probable stoichiometry of the discussed complexes is 1:1. As we can see in Table 1, the rest of the AmB polar groups are engaged in hydrogen-bond formation with DMPC to a considerably lower extent. The following expected trend can be also seen: the

farther from the polar head region the given AmB group is located, the smaller its participation in these interactions. Interestingly, the pattern of hydrogen bonds is quite similar in each of the simulated systems. This may suggest that the presence of sterols does not influence substantially the local abilities of the AmB headgroup to interact with other bilayer components.

However, if formation of these complexes really takes place inside the membrane, the above result can be interpreted only as a limitation of the simulation method. Unfortunately, the limited simulation time and relatively small values of diffusion constants for membrane components made it impossible to evaluate the possibility of primary complex formation. Nevertheless, several close contacts between antibiotic and sterol molecules were recorded in our simulations (especially one observed in the DMPC/Erg/AmB system, accompanied by a long-lasting intermolecular hydrogen bond between the Erg hydroxyl group and AmB OH-43). This finding seems to contradict the previous assumption that the charged groups of AmB are directly involved in the stabilization of the primary complex.⁵⁹ The relative position of AmB and sterol polar groups on the *z* axis together with steric effects suggest that hydroxyl groups OH-43, OH-13, or OH-11 of polyene (Figure 1) could be the key functional groups in AmB:sterol complex formation within the membrane interior. It is also worth mentioning here that AmB hydroxyl group OH-43 was previously found (simulation of the AmB channel)²⁰ to participate in the chain of hydrogen bonds between the antibiotic molecules within the channel. The importance of these groups agrees with the assumptions made by Matsumori et al. in their study on certain AmB derivatives, which appear to have a higher affinity toward Erg than the parent antibiotic.⁶⁰ The calculations intended to estimate the stability and geometry of the AmB:sterol primary complexes are currently in progress and will be published elsewhere. It is also worth mentioning here that the lack of direct interaction between polyene and sterol molecules in the simulated systems implies that the differences in AmB properties (depending on the system composition), described in the preceding sections, are mainly due to different effects of both sterols on the structural and dynamical properties of the membrane (indirect sterol action).

Making reasonable assumptions, namely, that (i) the rigid structure of the AmB molecule is not highly sensitive to changes in the surrounding environment, (ii) loss of rotational and translational entropy upon transfer of the AmB molecule from the *ld* to *lo* phase is negligible, and (iii) AmB affects in a similar way the structure of the lipid bilayer in the *ld* and the *lo* phase state, we can expect that the free energy of AmB transfer from the *ld* domain to the sterol-rich *lo* domain will be dominated by the enthalpic term, that is, by the difference in potential energy of interaction between antibiotic and its surroundings. Therefore, we estimated the relative affinity of AmB for different membrane environments simply by calculating the average energy of interaction between the AmB molecule and the rest of the molecules in the three simulated systems. Using a cutoff of 1.5 nm for nonbonded energy terms (both electrostatic and van der Waals interactions), we obtained values of –1093.7, –1109.0, and –1119.3 kJ/mol as the average interaction energy in DMPC/AmB, DMPC/Chol/AmB, and DMPC/Erg/AmB systems, respectively. Subtracting appropriate values, we finally obtained the energy differences accompanying AmB translocation from pure DMPC to DMPC/Chol bilayer (–15.3 kJ/mol) and to DMPC/Erg bilayer (–25.6 kJ/mol). Apparently, these data support the previous observations made in experi-

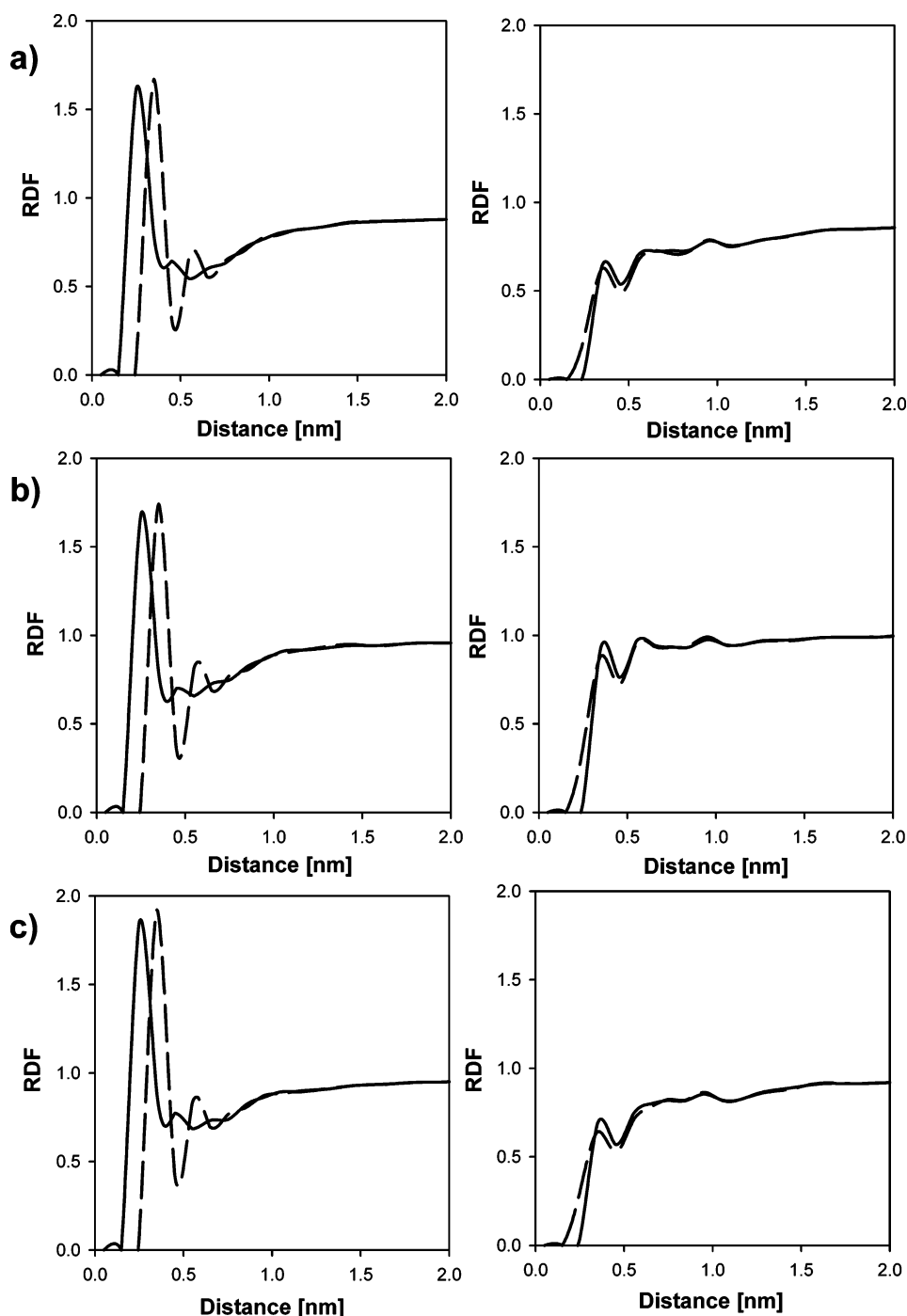


Figure 8. Three-dimensional radial distribution functions of water oxygen (dashed line) and hydrogen (solid line) atoms around the C atom of AmB carboxyl group (left) and the N atom of the AmB amino group (right) calculated from simulation of the DMPC/AmB (a), DMPC/Chol/AmB (b), and DMPC/Erg/AmB (c) systems.

ments that AmB and other rigid polyene molecules, like nystatin, exhibit higher affinity toward ordered lipid bilayers (e.g., in gel phase) than disordered lipid phases.^{61,62} Moreover, our results indicate that the corresponding equilibrium constant (i.e., partition coefficient) can be greater in Erg-containing fungal cell membranes than in human cell membranes with Chol. If we consider that antibiotic molecules seem to more strongly restrict the conformational freedom of phospholipid acyl chains in a pure bilayer than in already ordered *lo* phases (for example, see a very small effect of AmB presence on S_{CD} in highly ordered DMPC/Erg bilayer in Figure 5c), the discussed partition coefficients could be even higher than estimated from interaction energy differences.

We also investigated differences in the hydration pattern of antibiotic molecules in the three simulated systems. Using the same hydrogen-bond criterion as above, it was found that the AmB molecule makes on average 6.04 ± 0.42 , 6.31 ± 0.50 , and 6.27 ± 0.47 hydrogen bonds with water molecules in the DMPC/AmB, DMPC/Chol/AmB, and DMPC/Erg/AmB system, respectively. The calculated values are very close to those obtained for DMPC molecules in the systems without antibiotic (in the same order 6.5 ± 0.14 , 6.0 ± 0.11 , and 6.0 ± 0.12),¹⁶ implying a similar level of solvation of the polar headgroups of both molecules. However, the opposite effect of sterol presence on the molecules hydration can be observed. Namely, bilayer condensation is accompanied by a small reduction of

water penetration to DMPC headgroups. On the contrary, we observe a slight increase of AmB hydration in the more ordered sterol-containing membranes probably arising from a noticeable shift of antibiotic molecules toward the water phase (see also Figure 3).

Efforts to improve the selective toxicity of AmB are focused especially on chemical modifications of two ionized groups of the antibiotic.^{10,11} Therefore, hydration of these groups is of primary importance since it might affect, for example, the thermodynamics and kinetics of the transfer from the water phase to the lipid bilayer and the preferred location of antibiotic molecules inside the membrane. To compare the hydration of the AmB's ionized groups in each of the studied membrane environments, we calculated the three-dimensional radial distribution functions (RDF) of water oxygen and hydrogen atoms around the central atoms of both functional groups (i.e., the N atom in NH_3^+ and the C atom in COO^- group). The calculated RDFs (Figure 8) unequivocally show that irrespective of the bilayer composition a similar difference occurs in the solvation level of both considered groups. In all systems the carboxyl group, as a part of the AmB molecule being most strongly exposed to the water phase, is significantly hydrated and thus can be recognized as a specific anchor that binds the macrolide moiety to the water/membrane interface. On the contrary, NH_3^+ interacts with water molecules very weakly, which is most probably a consequence of its direct involvement in the interaction with PO_4^- groups of phospholipids. The above findings make it possible to interpret the experimentally demonstrated growth of AmB selectivity under esterification of its carboxyl group (e.g., AmB methyl ester⁶³ and second generation of AmB derivatives^{10,64}). It seems that the decrease of carboxyl group polarity should lead to deeper embedding of the polyene molecule within the membrane. Due to the fact that differences in the physicochemical properties of the Erg- and Chol-containing lipid bilayer are concentrated especially in the hydrocarbon core region of the membrane,¹⁶ deeper location of the antibiotic should favor differentiation of its behavior and, in the context of our hypothesis, increase its selective toxicity. In particular, weaker interactions with a polar interface would most likely enlarge the differences in the dynamic properties of antibiotic molecules and especially in amplitudes and rates of their wobbling motion. These changes may, in turn, not allow for effective channel formation in the less ordered Chol-containing phospholipid bilayer.

Conclusions

To obtain detailed insight into AmB behavior inside its molecular target as well as challenge the hypothesis about the indirect (modulation of the membrane properties) or direct (involvement in the complex with the antibiotic) role of sterols in the formation of the AmB channel, three model membrane systems containing AmB were studied and extensive analysis of the antibiotic behavior as well as the properties of the membrane itself was carried out. The following conclusions can be drawn.

As far as the differences between sterol-rich and sterol-free membranes are concerned, our results show that in the former systems almost all AmB monomers reside only in one membrane leaflet; whereas in pure phospholipid bilayer significant penetration of the second layer by AmB is observed. This effect, mainly a consequence of different thickness of sterol-containing and sterol-free membranes, might be related to the previously postulated ability of AmB to create so-called single- and double-length channels. However, this is only a proposition because

we did not observe in our simulations the direct interaction between AmB molecules residing in the opposite leaflets of the bilayer.

In the sterol-free system it was also found that AmB increases the conformational order of neighboring phospholipid molecules. This finding suggests that formation of AmB-rich domains, observed experimentally in lipid membranes,⁵⁰ may occur in a way analogous to the sterol-induced separation of the *lo* phases. On the other hand, existence of the antibiotic-enriched ordered domains, which should promote channel formation, could explain the channel-type ionophoric action of AmB in sterol-free bilayers at high antibiotic concentration.⁶⁵

Concerning sterol-rich systems, it has been found that the presence of a physiological amount of sterols (both Chol and Erg) in the lipid bilayer induces a change of AmB position in such a way that the molecule becomes oriented much more perpendicularly to the membrane surface (this is also in agreement with experimental data¹³). The presence of sterol molecules in the membrane additionally significantly influences the behavior of antibiotic molecules decreasing the rate and range of different modes of their motion. It can be postulated that this effect, especially reduction of wobbling motions amplitudes inside the sterol-induced *lo* phases, should facilitate or even enable the channel formation process. Thus, our results support the assumption of indirect sterol action in expressing AmB ionophoric activity. The presence of strong and specific AmB–phospholipid interactions in all three studied systems also supports the idea of an indirect role of sterol in channel formation. It was found that AmB's NH_3^+ group forms specific and long-lasting hydrogen bonds with DMPC's PO_4^- groups. These interactions are responsible for creation of the AmB: phospholipid complex with 1:1 stoichiometry (also observed experimentally^{41,58}). In this case, sterol is only needed to modify the fluidity of the membrane and, therefore, help AmB to adopt the proper orientation/position required for channel formation. It is also worth mentioning here that AmB was previously shown to permeabilize sterol-free lipid bilayers in their gel phase.^{66,67} Thus, this observation also confirms that the presence of a relatively rigid and ordered lipid environment may be necessary for formation of the stable channel structure.

Concerning differences of AmB behavior in both sterol-containing membranes (Chol or Erg), it has been observed that the type of sterol significantly affects the dynamic properties of the embedded antibiotic molecules. In particular, Erg, which has been shown to induce a higher order in the lipid bilayer, reduces the amplitude and rate of the AmB wobbling motion slightly stronger than Chol. Such behavior should favor channel formation and/or its stabilization. Thus, differentiation of AmB wobbling dynamics, depending on the type of sterol present in the bilayer, might be proposed as one of the molecular reasons for different ionophoric action of the antibiotic in both types of membranes (i.e., selective action of AmB). Another interesting observation, which may be interpreted in the context of AmB selectivity, was finding that the antibiotic increases the internal order of DMPC bilayer containing 25 mol % of Chol while it has no effect on the order of the bilayer with the same amount of Erg. Therefore, one could propose that the different effect of both sterols on phospholipid physicochemical properties revealed by us and recently established in other studies^{16,68–70} (especially the higher ability of Erg to induce molecular order in lipid bilayer) may play a crucial role in differentiating the biological action of AmB in both membrane types.

Finally, it is worth stressing that performed calculations suggest that relatively rigid and elongated AmB molecules

exhibit higher affinity toward the sterol-containing *lo* phases and, therefore, may be cumulated in ordered membrane domains (e.g., lipid rafts). Since the partition coefficient between the *ld* and *lo* phase appears to be greater in the case of the Erg-containing membrane compared to the Chol-containing equivalent, this effect can be also discussed as the possible origin of AmB-selective toxicity and indirect sterol involvement in expression of AmB activity.

Acknowledgment. The authors acknowledge financial support by the Ministry of Education and Science (grant no. 3 P05F 012 25) and Gdansk University of Technology (Poland). The authors also thank the TASK Computational Center (Gdansk, Poland) for granting CPU time.

References and Notes

- Gallis, H. A.; Drew, R. H.; Pickard, W. W. *Rev. Infect. Dis.* **1990**, *12*, 308–329.
- Cereghetti, D. M.; Carreira, E. M. *Synthesis (Stuttgart)* **2006**, 914–942.
- Bolard, J. *Biochim. Biophys. Acta* **1986**, *864*, 257–304.
- Brajtburg, J.; Powderly, W. G.; Kobayashi, G. S.; Medoff, G. *Antimicrob. Agents Chemother.* **1990**, *34*, 183–188.
- Teerlink, T.; De Kruijff, B.; Demel, R. A. *Biochim. Biophys. Acta* **1980**, *599*, 484–492.
- Kerridge, D. *Adv. Microb. Physiol.* **1986**, *27*, 1–72.
- Fournier, I.; Barwicz, J.; Tancrede, P. *Biochim. Biophys. Acta: Biomembr.* **1998**, *1373*, 76–86.
- Deray, G. *J. Antimicrob. Chemother.* **2002**, *49*, 37–41.
- Prendergrast, M. M.; Tong, K. B. *Clin. Infect. Dis.* **2003**, *37*, 1396.
- Szinder-Richert, J.; Mazerski, J.; Cybulska, B.; Grzybowska, J.; Borowski, E. *Biochim. Biophys. Acta: Gen. Subj.* **2001**, *1528*, 15–24.
- Borowski, E. *Farmaco* **2000**, *55*, 206–208.
- Hartel, S. C.; Hatch, C.; Ayenew, W. J. *Liposome Res.* **1993**, *3*, 377–408.
- Lopes, S.; Castanho, M. A. R. B. *J. Phys. Chem. B* **2002**, *106*, 7278–7282.
- Dynarowicz-Latka, P.; Seoane, R.; Minones, J.; Velo, M.; Minones, J. *Colloid Surf. B* **2003**, *27*, 249–263.
- Coutinho, A.; Silva, L.; Fedorov, A.; Prieto, M. *Biophys. J.* **2004**, *87*, 3264–3276.
- Czub, J.; Baginski, M. *Biophys. J.* **2006**, *90*, 2368–2382.
- Fujii, G.; Chang, J. E.; Coley, T.; Steere, B. *Biochemistry* **1997**, *36*, 4959–4968.
- Gagos, M.; Koper, R.; Gruszecki, W. I. *Biochim. Biophys. Acta: Biomembr.* **2001**, *1511*, 90–98.
- De Kruijff, B.; Demel, R. A. *Biochim. Biophys. Acta* **1974**, *339*, 57–70.
- Baginski, M.; Resat, H.; McCammon, J. A. *Mol. Pharmacol.* **1997**, *52*, 560–570.
- Baginski, M.; Resat, H.; Borowski, E. *Biochim. Biophys. Acta: Biomembr.* **2002**, *1567*, 63–78.
- Feller, S. E. *Curr. Opin. Colloid Interface Sci.* **2000**, *5*, 217–223.
- Scott, H. L. *Curr. Opin. Struct. Biol.* **2002**, *12*, 495–502.
- Koubi, L.; Saiz, L.; Tarek, M.; Scharf, D.; Klein, M. L. *J. Phys. Chem. B* **2003**, *107*, 14500–14508.
- Pasenkiewicz-Gierula, M.; Rog, T.; Grochowski, J.; Serda, P.; Czarnecki, R.; Librowski, T.; Lochynski, S. *Biophys. J.* **2003**, *85*, 1248–1258.
- LaRocca, P.; Biggin, P. C.; Tieleman, D. P.; Sansom, M. S. P. *Biochim. Biophys. Acta: Biomembr.* **1999**, *1462*, 185–200.
- Mihailescu, D.; Smith, J. C. *Biophys. J.* **2000**, *79*, 1718–1730.
- Sternal, K.; Czub, J.; Baginski, M. *J. Mol. Model.* **2004**, *10*, 223–232.
- Faraldo-Gomez, J. D.; Smith, G. R.; Sansom, M. S. P. *Eur. Biophys. J. Biophys. Lett.* **2002**, *31*, 217–227.
- Baginski, M.; Gariboldi, P.; Bruni, P.; Borowski, E. *Biophys. Chem.* **1997**, *65*, 91–100.
- Lindahl, E.; Hess, B.; van der Spoel, D. *J. Mol. Model.* **2001**, *7*, 306–317.
- Berger, O.; Edholm, O.; Jahnig, F. *Biophys. J.* **1997**, *72*, 2002–2013.
- Hofsass, C.; Lindahl, E.; Edholm, O. *Biophys. J.* **2003**, *84*, 2192–2206.
- Schuettelkopf, W.; Van Alten, D. M. F. *Acta Crystallogr., Sect. D: Biol. Cryst.* **2004**, *60*, 1355–1363.
- Resat, H.; Baginski, M. *Eur. Biophys. J. Biophys. Lett.* **2002**, *31*, 294–305.
- Baginski, M.; Borowski, E. *Theochem—J. Mol. Struct.* **1997**, *389*, 139–146.
- Essmann, U.; Perera, L.; Berkowitz, M. L.; Darden, T.; Lee, H.; Pedersen, L. G. *J. Chem. Phys.* **1995**, *103*, 8577–8593.
- Hess, B.; Bekker, H.; Berendsen, H. J. C.; Fraaije, J. G. E. M. *J. Comput. Chem.* **1997**, *18*, 1463–1472.
- Miyamoto, S.; Kollman, P. A. *J. Comput. Chem.* **1992**, *13*, 952–962.
- Berendsen, H. J. C.; Postma, J. P. M.; Dinola, A.; Haak, J. R. *J. Chem. Phys.* **1984**, *81*, 3684–3690.
- Matsuoka, S.; Ikeuchi, H.; Matsumori, N.; Murata, M. *Biochemistry* **2005**, *44*, 704–710.
- Vertut-Croquin, A.; Bolard, J.; Chabbert, M.; Gary-Bobo, C. M. *Biochemistry* **1983**, *22*, 2939–2944.
- Coutinho, A.; Prieto, M. *Biophys. J.* **2003**, *84*, 3061–3078.
- Akutsu, H.; Nagamori, T. *Biochemistry* **1991**, *30*, 4510–4516.
- Ohvo-Rekila, H.; Ramstedt, B.; Leppimäki, P.; Slotte, J. P. *Prog. Lipid Res.* **2002**, *41*, 66–97.
- Urbina, J. A.; Pekerar, S.; Hong-biao, L.; Patterson, J.; Montez, B.; Oldfield, E. *Biochim. Biophys. Acta: Biomembr.* **1995**, *1238*, 163–176.
- Chazalet, M. S. P.; Thomas, C.; Dupeyrat, M.; Gary-Bobo, C. M. *Biochim. Biophys. Acta* **1988**, *944*, 477–486.
- Smondryev, A. M.; Berkowitz, M. L. *Biophys. J.* **1999**, *77*, 2075–2089.
- Maertens, J. A.; Boogaerts, M. A. *Curr. Pharm. Design* **2000**, *6*, 225–239.
- Milhaud, J.; Michels, B. *Chem. Phys. Lipids* **1999**, *101*, 223–235.
- Mouritsen, O. G.; Jorgensen, K. *Chem. Phys. Lipids* **1994**, *73*, 3–25.
- Bolard, J.; Legrand, P.; Heitz, F.; Cybulska, B. *Biochemistry* **1991**, *30*, 5707–5715.
- Lipari, G.; Szabo, A. *J. Am. Chem. Soc.* **1982**, *104*, 4546–4559.
- Venable, R. M.; Zhang, Y. H.; Hardy, B. J.; Pastor, R. W. *Science* **1993**, *262*, 223–226.
- Szabo, A. *J. Chem. Phys.* **1984**, *81*, 150–167.
- Filippov, A.; Oradd, G.; Lindblom, G. *Langmuir* **2003**, *19*, 6397–6400.
- Almeida, P. F. F.; Vaz, W. L. C.; Thompson, T. E. *Biochemistry* **1992**, *31*, 6739–6747.
- Minones, J.; Minones, J.; Conde, O.; Patino, J. M. R.; Dynarowicz-Latka, P. *Langmuir* **2002**, *18*, 2817–2827.
- Herve, M.; Debouzy, J. C.; Borowski, E.; Cybulska, B.; Gary-Bobo, C. M. *Biochim. Biophys. Acta* **1989**, *980*, 261–272.
- Matsumori, N.; Sawada, Y.; Murata, M. *J. Am. Chem. Soc.* **2005**, *127*, 10667–10675.
- Bolard, J.; Vertut-Croquin, A.; Cybulska, B.; Gary-Bobo, C. M. *Biochim. Biophys. Acta* **1981**, *647*, 241–248.
- Coutinho, A.; Prieto, M. *Biophys. J.* **1995**, *69*, 2541–2557.
- Racis, S. P.; Plescia, O. J.; Geller, H. M.; Schaffner, C. P. *Antimicrob. Agents Chemother.* **1990**, *34*, 1360–1365.
- Slisz, M.; Cybulska, B.; Mazerski, J.; Grzybowska, J.; Borowski, E. *J. Antibiot.* **2004**, *57*, 669–678.
- Cotero, B. V.; Rebollo-Antunez, S.; Ortega-Blake, I. *Biochim. Biophys. Acta: Biomembr.* **1998**, *1375*, 43–51.
- HsuChen, C. C.; Feingold, D. S. *Biochem. Biophys. Res. Commun.* **1973**, *51*, 972–978.
- Scott, J.; Ruckwardt, T.; Hartel, S. C. *FASEB J.* **1997**, *11*, 1429.
- Hsueh, Y. W.; Gilbert, K.; Trandum, C.; Zuckermann, M.; Thewalt, J. *Biophys. J.* **2005**, *88*, 1799–1808.
- Bernsdorff, C.; Winter, R. *J. Phys. Chem. B* **2003**, *107*, 10658–10664.
- Gabrielska, J.; Gagos, M.; Gubernator, J.; Gruszecki, W. I. *FEBS Lett.* **2006**, *580*, 2677–2685.